

# Radionuclide Content of Sands Used for Construction in Kakamega County, Kenya and Associated Indoor Radon Diffusion Fluxes

Shikali Collins<sup>1\*</sup> Munji Mathew<sup>1</sup> Ambusso Willis<sup>1</sup>

1. Department of Physics, Kenyatta University, P.O. Box 43844, Nairobi, Kenya

\* E-mail of the corresponding author: [cshikali@gmail.com](mailto:cshikali@gmail.com)

## Abstract

Studies have been carried out to determine the natural radioactivity in construction sand and their associated radiation hazard in the old gold mining belt of Kakamega County, Kenya. The radioactivity concentrations of  $^{226}\text{Ra}$ ,  $^{232}\text{Th}$  and  $^{40}\text{K}$  were measured using a gamma ray spectrometer with a NaI(Tl) detector. The results of concentrations of naturally occurring radionuclides were as follows:  $^{226}\text{Ra}$  ranged from  $36.79 \pm 8.89$  to  $185.21 \pm 5.89 \text{ Bqkg}^{-1}$ ,  $^{232}\text{Th}$  ranged from  $322.38 \pm 2.56$  to  $158.92 \pm 7.95 \text{ Bqkg}^{-1}$  and  $^{40}\text{K}$  ranged from  $322.38 \pm 16.12$  to  $960.53 \pm 48.03 \text{ Bqkg}^{-1}$ . The radium equivalent activities and the radiation hazard index associated with the natural radionuclides were calculated. A computer program was developed and applied to estimate the diffused indoor radon concentration by solving a simple transport equation. The indoor radon was assumed to originate from the walls of a room constructed from sands rich in uranium minerals found in this region.

**Keywords:** Radioactivity; Radium; Thorium; Potassium; Building sand; Indoor radon

## 1. Introduction

The building sands around the old gold mining zones in Kakamega County are potential source of radon, since they contain relatively high radium activity concentration ( $>40 \text{ Bqkg}^{-1}$ ) (UNSCEAR, 1993). Building materials are known sources of airborne radioactivity and external radiation from the decay series of Uranium (Al-jarallah, 2001). Exhalation of radon ( $^{222}\text{Rn}$ ) from these materials is of great importance since the short-lived decay products of radon are the largest contributors to the lung dose of inhaled radionuclides (Paredes et al., 1987).

Indoor radon is released from radium trapped in mineral grains of the building materials and soil. The gas then escapes to the indoor air by diffusion and/or advection. Hence, a study of the diffusion of the radon will provide a greater insight of its possible pathways through the walls constructed from sand into the surrounding air in a room (Spleenman et al., 2009). The harmful effects of gamma- radiation from building materials and radon in dwellings are generally well known, but information on concentration levels of radon in dwellings and workplaces in Kenya is not readily available. Thus the measurement and modeling of radon concentration fluxes in dwellings can be helpful in identifying potential environmental hazardous areas in the region.

Many techniques for measuring indoor radon have been developed. In this study a theoretical model to estimate the contribution of mineral sands used for construction to the indoor dose rate and to radon air contribution is posed. To validate the model, indoor radon concentrations measured from different monitoring stations were compared with the model results.

## 2 Material and methods

### 2.1 Experimental Procedures

Nine sand samples were collected along the banks of R. Yala and ten samples along the R. Isiukhu in the gold mining zones of Kakamega County, Kenya as shown in Fig.1. The samples were dried, ground, accurately weighed ( $500 \pm 0.1 \text{ g}$ ) and placed in sealed plastic bags for four weeks prior counting. This was for the samples to attain nearly secular equilibrium between long lived parents ( $^{226}\text{Ra}$ ,  $^{232}\text{Th}$ ,  $^{40}\text{K}$ ) and their shorter lived daughters.

The gamma ray measurements were then carried out using 76mm x 76mm NaI(Tl) detector having an energy resolution of 7.03% and relative efficiency of 75% at 662 KeV line of  $^{137}\text{Cs}$ . The samples were then placed on a lead shielded calibrated detector ready for counting. Energy calibration involved measuring sources that emits gamma rays of known energy and comparing the measured peaks with energy. In this work, IAEA certified reference materials ( a standard soil of known radioactivity, soil 6, uranium ore sample, RGU1 and a thorium ore sample RGTh1) were used and calibration done in energy range of 350 KeV to 3000 KeV.

In determination of the gamma activities of the natural radionuclides in the samples, the focus was placed on the identification of three regions of interest (Roi) in the spectrum, which were centered on the three characteristic photo-peaks, at approximate 1460 keV ( $^{40}\text{K}$ ), 1765 keV ( $^{214}\text{Bi}$ ) and 2615 keV ( $^{208}\text{Tl}$ ). These were used to evaluate activity levels of  $^{40}\text{K}$ ,  $^{226}\text{Ra}$  and  $^{232}\text{Th}$  series, respectively (Suresh et al., 2011). Average background count was subtracted from the sample count to obtain the net count (two background readings were taken at the end of two weeks for 8 hours each).

The activity of  $^{226}\text{Ra}$ ,  $^{232}\text{Th}$  or  $^{40}\text{K}$  was calculated using the following relation:

$$\frac{A_s \cdot M_s}{I_s} = \frac{A_R \cdot M_R}{I_R} \quad (1)$$

where,  $A_S$  is the activity of the radionuclide in the sample,  $M_S$ , is the mass of the sample to be analyzed,  $I_S$  is the intensity of the radionuclide in the sample to be analyzed,  $A_R$  is the activity of the radionuclide in the reference sample,  $M_R$  is the mass of the reference sample,  $I_R$  is the intensity of the radionuclide in the reference sample. Several spectra for all samples were recorded and stored in text files of a PC based MCA ready for a detailed analysis.

### 2.2 modeling of radon diffusion concentration fluxes in dwelling space

The model was used to estimate and predict the concentration of indoor radon emitted from walls in dwellings constructed from sand. This was aimed at formulation of effective control strategies to reduce emission of radon in living space. The model assumes that radon is not released from materials inside the room, it is homogeneously mixed with the room air and it does not react or disappear by any process other than decay (Anjos et al., 2011).

The variation of radon in an enclosed space can be described by a mass conservation equation (Man C.K. and Yeung H.S., 1999). Then, the radon concentration can be obtained by solving the differential equation:

$$\frac{\partial C}{\partial t} = \frac{S}{V} - \lambda_{Rn} C + \frac{q}{V} \quad (2)$$

where  $C$  is the concentration of radon ( $Bqm^{-3}$ ),  $S$  is the creation rate of radon,  $V$  is the volume of the room ( $m^3$ ),  $\lambda_{Rn}$  is the decay constant of radon ( $7.54 \times 10^{-3} h^{-1}$ ) and  $q$  is the radon flux density ( $Bqm^{-2}h^{-1}$ ).

Equation 2 is solved for given boundary conditions i.e.  $C$  is set to some fixed value (for example, zero at the walls constructed from sand-air interface and maximum as radon diffuses further in the room). Explicit finite difference numerical method was employed in solving equation 2. A computational grid was defined for the problem, the equation 2 transformed into one large matrix equation as shown by Eq. 3;

$$C_j^{n+1} = C_j^n + \frac{S}{V} \Delta t - \lambda_{Rn} \Delta t C_j^n + \frac{D}{V} \Delta t \sum \left( \frac{C_{j+1}^n - 2C_j^n + C_{j-1}^n}{(\Delta x)^2} \right) \quad (3)$$

where indexes  $j$  and  $n$  refer to the discrete position and times determined by step lengths  $\Delta x$  and  $\Delta t$  for the coordinates  $x$  and time  $t$  respectively

The unknowns being concentrations and the matrix coefficients depended on the grid, material properties and boundary conditions.

### 2.3 Calculation of radiological effects:

#### 2.3.1 Dose rate calculation;

The absorbed dose rate was calculated from the measured activities of  $^{226}Ra$ ,  $^{232}Th$  and  $^{40}K$  in the sand samples from the study region using Eq. 4 below (UNCEAR, 2000);

$$D(nGyh^{-1}) = 0.462C_{Ra} + 0.604C_{Th} + 0.042C_K \quad (4)$$

Where  $D$  is the absorbed dose rate ( $nGyh^{-1}$ ).  $C_{Ra}$ ,  $C_{Th}$  and  $C_K$  are activity concentrations ( $Bqkg^{-1}$ ) of  $^{226}Ra$ ,  $^{232}Th$  and  $^{40}K$  respectively. In estimation of annual effective dose rates (AEDR), the conversion coefficient from absorbed dose to effective dose,  $0.7 SvGy^{-1}$  and in door occupancy factor of 0.8 (UNCEAR, 2000) were used. Thus the effective dose rate was calculated by the Eq. 5 below;

$$AEDR \left( \frac{mSv}{y} \right) = D \left( \frac{nGy}{h} \right) \times 8760 \left( \frac{h}{y} \right) \times 0.8 \times 0.7 \left( \frac{Sv}{Gy} \right) \times 10^{-6} \quad (5)$$

#### 2.3.2 Calculation of hazard indexes;

To limit the radiation dose to permissible dose equivalent limit of  $1 mSvy^{-1}$ , the external hazard index ( $H_{ex}$ ) was calculated using Eq. 6:

$$H_{ex} = \frac{C_{Ra}}{370} + \frac{C_{Th}}{259} + \frac{C_K}{4810} \leq 1 \quad (6)$$

Another index, Gamma index ( $I_\gamma$ ), which is a criterion for assessment of the radiological suitability of a building material defined by the European Commission (EC, 1999) was calculated by the following formula:

$$I_{\gamma} = \frac{A_{Ra}}{300} + \frac{A_{Th}}{200} + \frac{A_K}{3000} \quad (7)$$

### 3 Results and discussion

#### 3.1 Radioactivity of building sand assessment results

Table 1 shows the measured radioactivity concentrations of  $^{226}\text{Ra}$ ,  $^{232}\text{Th}$  and  $^{40}\text{K}$  in sand samples, which were collected along the banks of rivers Isiukhu and Yala in old gold mining zones of Kakamega County, Kenya. From the table, the activity concentration ranged from  $36.79 \pm 2.03$  to  $185.21 \pm 5.89$   $\text{Bqkg}^{-1}$  for  $^{226}\text{Ra}$ ,  $51.12 \pm 5.89$  to  $158.92 \pm 7.95$   $\text{Bqkg}^{-1}$  for  $^{232}\text{Th}$  and  $322.38 \pm 16.12$  to  $960.53 \pm 40.08$   $\text{Bqkg}^{-1}$  for  $^{40}\text{K}$ . The maximum activity concentration of  $^{226}\text{Ra}$  ( $185.21 \pm 5.89$   $\text{Bqkg}^{-1}$ ) and  $^{232}\text{Th}$  ( $158.92 \pm 7.95$   $\text{Bqkg}^{-1}$ ) were observed in Mukhonje (S2) and Lwanungu (S15) respectively. This might be attributed to heavy artisanal gold mining activities in these places. During mining process concealed radioactive rich granite rocks, sandstones, monazites and gold bearing quartzite rocks common in the region are broken down and dispersed by the river water.

The lowest concentration of the radionuclides was found at Eshibakala (S8), Ematsayi (S6) and Esalasala (S7) which may be due to high composition of silica in the sands (Ramasamy et al., 2009). For comparison purposes, data published for activity concentration of  $^{226}\text{Ra}$ ,  $^{232}\text{Th}$  and  $^{40}\text{K}$  in sand for some countries is given in table 2.

Table 3 presents the radium equivalent activity, absorbed dose rate, annual effective dose equivalent and external hazard index for the sand samples. The calculated radium equivalent activity in the studied sand samples varied from  $207.38$   $\text{Bqkg}^{-1}$  (S8) to  $397.62$   $\text{Bqkg}^{-1}$  (S19) with a mean of  $321.67 \pm 12.4$   $\text{Bqkg}^{-1}$ . The calculated absorbed dose rate ranged from  $99.6$  (S8) to  $186.84$  (S19) with a mean of  $151.76 \pm 5.65$   $\text{nGyh}^{-1}$ . The mean absorbed dose rate is found to be 2.98 times the world average value  $51$   $\text{nGyh}^{-1}$ , (UNCEAR, 2000). The calculated values of annual effective dose rate range from  $0.48$  to  $0.92$   $\text{mSv}$ , with a mean value of  $0.74$   $\text{mSv}$ . The calculated value of external hazard index ranges from  $0.57$  to  $1.09$  with a mean of  $0.88$ . Since the average value is lower than unity, according to European commission on radiation protection report (EC, 1999), sand from the study area is safe and can be used as construction material without posing any radiological threat to the public.

#### 3.2 Indoor radon model results

The diffusion equation was solved (within given boundary conditions) in section 2.2 and the solution of Eq. 3 gives the results plotted in Fig.2. From the curves, the radon atoms exhaled from the walls in a room increases exponential with time until radioactive secular equilibrium is reached. If there is leakage and/or back-diffusion of radon atoms as they diffuse from the wall surfaces, the exhalation is depressed. This results to the lowering of radon concentration equilibrium value as shown by curves 1 and 2 in Fig.2.

The model predicts indoor radon concentration of  $12.5$   $\text{Bqkg}^{-1}$  (without back-diffusion and leakage) and  $8.5$   $\text{Bqkg}^{-1}$  (with back-diffusion and leakage). For the purpose of validating the model, the indoor radon concentrations were measured in classrooms in the study region. The concentrations were measured using activated charcoal canisters. In general the model underestimated all the indoor radon concentrations as shown in Fig.3. This was attributed to ignoring other possible radon entry pathways in the room e.g. radon entry by the soil gas.

### 4 Conclusions

Activity levels of natural radionuclide of uranium, thorium and potassium in construction sand sampled from old gold mining zones of Kakamega County, a suspected High Background Radiation Area (HBRA), was measured. The radiological effects on humans due the natural radiations from sand were also estimated by use of radiological parameters. The measured mean activity concentration levels of  $^{226}\text{Ra}$ ,  $^{232}\text{Th}$  and  $^{40}\text{K}$  was found to be  $128.05 \pm 8.89$   $\text{Bqkg}^{-1}$ ,  $98.37 \pm 6.41$   $\text{Bqkg}^{-1}$  and  $756.39 \pm 35.99$   $\text{Bqkg}^{-1}$  respectively. These levels were found to be higher than worldwide accepted average values of  $50$ ,  $50$  and  $500$   $\text{Bqkg}^{-1}$  for  $^{226}\text{Ra}$ ,  $^{232}\text{Th}$  and  $^{40}\text{K}$  respectively (Ramasamy et al., 2009). The calculated external hazard and effective dose rate for the indoor radiation was found to range from  $0.57$ - $1.09$  and  $(0.48$ - $0.92)$   $\text{mSvy}^{-1}$  respectively. Basing on the recommended values, these results show that no intervention is necessary for the sands in the location under study.

A deterministic model was developed using conservation laws, taking into account diffusion, sources and decay of radon atoms in the indoor air. Differential equations that govern the transport of radon were set up and solved numerically using a computer code. Results of field measurement of indoor radon concentrations using passive detectors and simulated ones were compared. The results show that the model is capable of estimating radon flux densities in buildings.

#### Acknowledgement

The work described in this paper was supported by national council of science and technology grant.

## References

- Ackers J.G., den Boer J.F., de Jong P and Wolfschrijin N. (1985). Radioactivity and radon exhalation rates of building materials in Netherlands,. *Journal of Science of Total environment*, (45), 151-156.
- Al-jarallah, M. (2001). Radon exhalation from granites used in Saudi Arabia. *Journal of Environment Radioactivity* (53), 91-98.
- Anjos R.M., Ayub J.J. Cid A.S., Cardoso R. and Laceuda T. (2011). External gamma ray dose rate and radon concentration in indoor radon environments covered with Brazillian granites. *Journal of environmental Radioactivity* (102), 1055-1061.
- Cervic U., Damula N., Koby A.I., Celik N., Celik C. and Van A. (2009). Assessment of natural radioactivity of sand used in Turkey,. *Journal of Radiation Protection*, (29), 61-74.
- EC, European Commission. (1999). Radiation Protection Principles Concerning the natural radioactivity of building materials. *Directorate-General environment, nuclear safety and civil protection* .
- Hayumbu P., Zaman M.B., Lubaba N.C.H., Munsanje S.S. and Luleya D. (1985). Natural radioactivity in Zambian building materials and by-products. *Journal of applied radiation and Isotopes* (51), 93-96.
- Kumar V., Ramachandran T.V. and Prazad R. (1999). Natural radioactivity of Indian building materials and by-products. *Journal of applied radiation and Isotopes* , 93-96.
- Man C.K. and Yeung H.S. (1999). Modeling and measuring the indoor radon concentration in high rise buildings in Hong Kong. *Applied Radiation and Isotopes* (56), 1131-1135.
- Mustapha A.O, Narayan D.G.S., Patel G.P and Otswana D. (1997). Natural radioactivity in some building materials in Kenya and their contribution to the indoor external doses,. *Journal of radiation Protection and dosimetry* , I (71), 65-69.
- Ramasamy V., Suresh G., Meenakshisundaram V. and Gajendran V. (2009). Evaluation of natural radioisotope content in River sediments and excess lifetime cancer risk due to gamma radioactivity. *Research Journal of Environmental and Earth Sciences* , I (1), 6-10.
- Spleenman W.J., Lindasay R., Newman R.T. and de merjer R.J. (2009). radon generation and transport in and around a gold-mine tailing in S.A. *journal of radiation protection of the public and environment* .
- Suresh G. and Ramasamy V. (2011). A relationship between the natural radioactivity and mineralogy composition of the Ponnairyar river sediments, India. *Journal of environmental radioactivity* (102), 370-377.
- UNSCEAR. (2000). Sources and Effects of Ionising Radiation. *United Nation Scientific Committee On Effects of Atomic Radiation* .
- UNSCEAR. (1993). Exposure from natural sources of radiation. *United nation scientific committee on effects of atomic radiation* .
- Xinwei, L., and Xiaolan, Z.,. (2008). Radionuclide Content and associated hazards of building materials and by-products in Baoji, West China. *Journal of radiation protection dosimetry*, (128), 471-476.

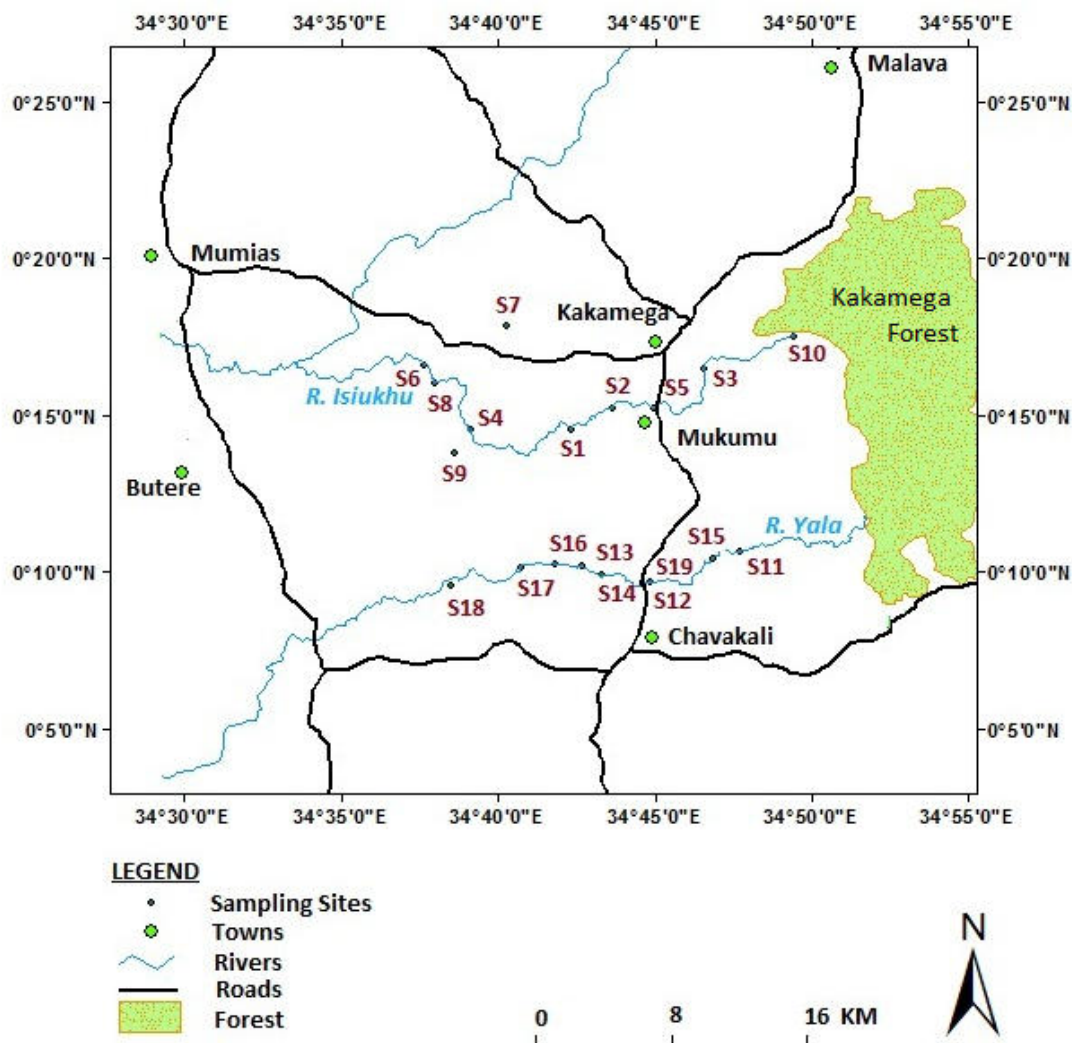


**Fig. 1:** A map showing the sampling sites in old gold mining region of Kakamega County

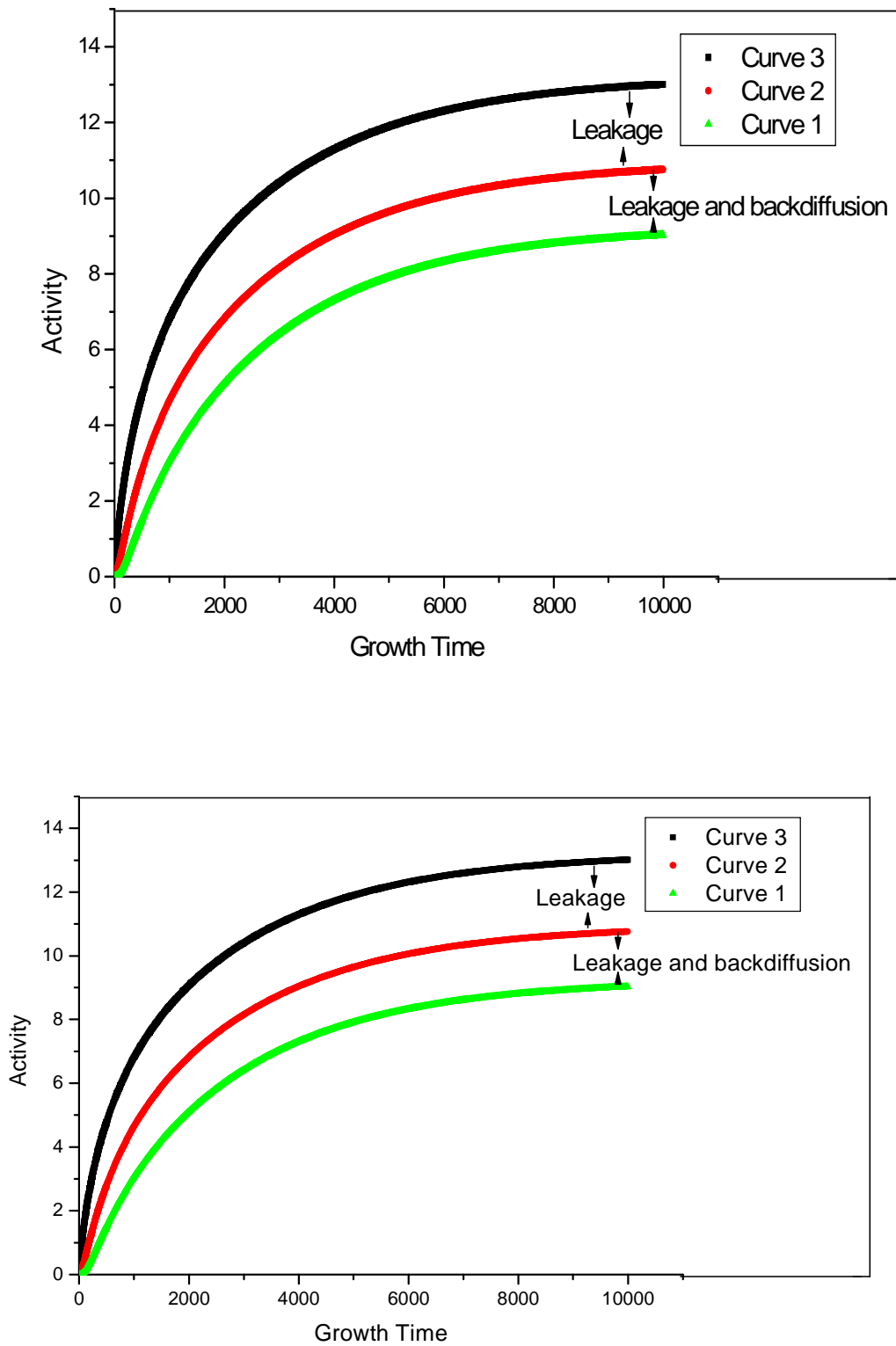
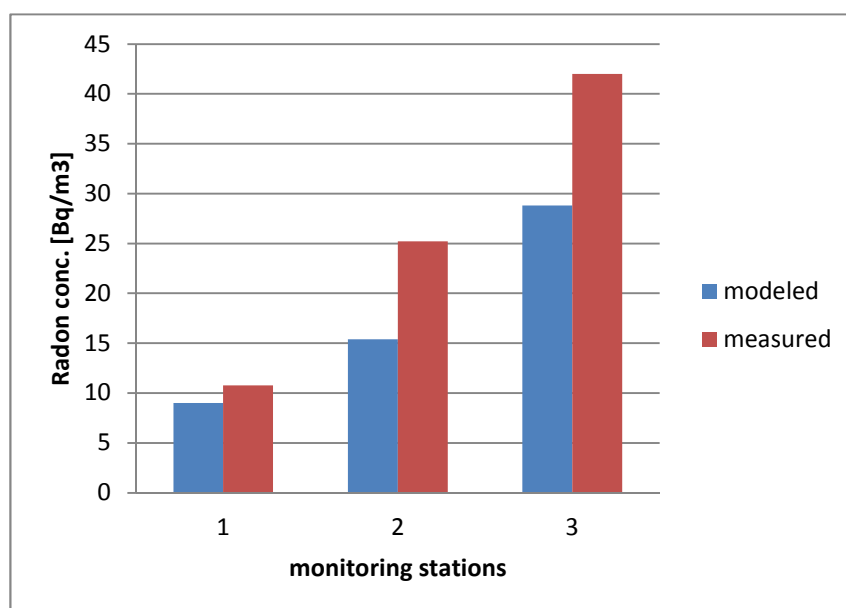


Fig.2. The modeled radon activity ingrowths in a closed room as a function of time





**Fig. 3:** A comparison of measured and modeled radon concentration in this work

**Table 1:** Specific  $\gamma$ -ray activity of <sup>226</sup>Ra, <sup>232</sup>Th and <sup>40</sup>K in the sand samples in this study

SITE	LOCATION	LATITUDE	LONGITUDE	<sup>226</sup> Ra (Bq/kg)	<sup>232</sup> Th (Bq/kg)	<sup>40</sup> K (Bq/kg)
S1	Shikhombelo	0.24223	34.70618	121.02±6.05	97.27±4.86	879.86±43.99
S2	Mukhonje	0.25406	34.72791	<b>185.21±9.26</b>	80.48±4.02	<b>960.53±48.03</b>
S3	Shieywe	0.27461	34.77672	107.92±5.40	87.28±4.36	812.68±40.63
S4	Mwibatsilu	0.24204	34.65198	89.45±4.47	62.53±3.13	821.89±41.10
S5	Kakamega	0.25396	34.75005	74.05±3.70	89.92±4.50	753.77±37.69
S6	Ematsayi	0.27671	34.62762	150.45±7.52	<b>51.12±2.56</b>	815.86±40.79
S7	Esalasala	0.29726	34.67118	155.29±7.76	95.05±4.75	<b>322.38±16.12</b>
S8	Eshibakala	0.26686	34.63300	<b>36.79±2.03</b>	82.11±4.11	760.00±38.00
S9	Imbale	0.22936	34.64335	163.38±8.17	75.90±3.70	696.11±34.81
S10	Mukulusu	0.29210	34.82379	118.48±5.92	96.15±4.81	485.36±24.29
S11	Shirulu	0.17712	34.79537	177.17±8.86	92.12±4.61	618.78±30.94
S12	Litambiza	0.16035	34.74432	138.02±6.90	84.90±4.25	877.98±43.90
S13	Shikokho	0.16993	34.71121	183.87±9.91	91.32±4.57	854.26±42.71
S14	Mwitabakha	0.16528	34.72227	99.98±5.00	100.69±5.03	648.13±32.41
S15	Lwanungu	0.17364	34.78089	115.10±5.76	<b>158.92±7.95</b>	725.21±36.26
S16	Isulu	0.17091	34.69703	108.55±5.43	142.28±7.11	778.95±38.95
S17	Bushiangala	0.16877	34.67945	113.26±5.66	147.15±7.36	762.68±38.13
S18	Ikonjero	0.15966	34.64159	143.14±7.46	105.15±5.26	914.99±45.75
S19	Iguhu	0.16097	34.74722	151.80±7.68	128.76±6.44	881.32±44.07
<b>Maximum</b>				185.21±5.89	158.92±7.95	960.53±48.03
<b>Minimum</b>				36.79±2.03	51.12±2.56	322.38±16.12
<b>Average</b>				128.05±8.89	98.37±6.41	756.39±35.99

**Table 2:** Average activity concentration of radionuclide in sand from old gold mining zones of Kakamega County compared to other parts of the world

Country	<sup>226</sup> Ra (Bqkg <sup>-1</sup> )	<sup>232</sup> Th (Bqkg <sup>-1</sup> )	<sup>40</sup> K (Bqkg <sup>-1</sup> )	References
Turkey	44	26	441	(Cervic et al., 2009)
Netherlands	8	11	200	(Ackers et al., 1985)
India	44	64	456	(Kumar et al., 1999)
China	23	36	891	(Xinwei, L., and Xiaolan, Z., 2008)
Zambia	24	26	714	(Hayumbu et al., 1985)
Kenya	11	5	802	(Mustapha et al, 1997)
Present study	128	98	756	

**Table 3:** Radium equivalent activity, external hazard index, dose rate and annual effective dose for sand samples in this work

Site no.	Ra <sub>eq</sub> (Bqkg <sup>-1</sup> )	Dose Rate (nGyh <sup>-1</sup> )	Annual Effective Dose (mSvy <sup>-1</sup> )	External Hazard index
S1	321.71	152.95	0.75	0.88
S2	367.53	175.47	0.86	1.01
S3	289.62	137.88	0.68	0.79
S4	236.40	114.31	0.56	0.65
S5	121.43	121.43	0.59	0.70
S6	280.66	135.13	0.66	0.77
S7	313.78	144.31	0.71	0.85
S8	<b>207.38</b>	<b>99.60</b>	<b>0.48</b>	<b>0.57</b>
S9	320.64	151.58	0.74	0.87
S10	289.94	134.73	0.66	0.79
S11	352.21	162.86	0.81	0.96
S12	320.88	153.00	0.75	0.88
S13	374.25	177.20	0.86	1.02
S14	289.33	135.75	0.67	0.79
S15	393.12	182.20	0.89	1.07
S16	366.53	171.03	0.83	1.00
S17	377.07	175.57	0.86	1.03
S18	357.55	169.51	0.83	0.98
S19	<b>397.62</b>	<b>186.84</b>	<b>0.92</b>	<b>1.09</b>
<b>Maximum</b>	<b>397.62</b>	<b>186.84</b>	<b>0.92</b>	<b>1.09</b>
<b>Minimum</b>	<b>207.38</b>	<b>99.6</b>	<b>0.48</b>	<b>0.57</b>
<b>Mean</b>	<b>321.67±12.4</b>	<b>151.76±5.65</b>	<b>0.74±0.02</b>	<b>0.88±0.03</b>



The IISTE is a pioneer in the Open-Access hosting service and academic event management. The aim of the firm is Accelerating Global Knowledge Sharing.

More information about the firm can be found on the homepage:  
<http://www.iiste.org>

## CALL FOR JOURNAL PAPERS

There are more than 30 peer-reviewed academic journals hosted under the hosting platform.

**Prospective authors of journals can find the submission instruction on the following page:** <http://www.iiste.org/journals/> All the journals articles are available online to the readers all over the world without financial, legal, or technical barriers other than those inseparable from gaining access to the internet itself. Paper version of the journals is also available upon request of readers and authors.

## MORE RESOURCES

Book publication information: <http://www.iiste.org/book/>

## IISTE Knowledge Sharing Partners

EBSCO, Index Copernicus, Ulrich's Periodicals Directory, JournalTOCS, PKP Open Archives Harvester, Bielefeld Academic Search Engine, Elektronische Zeitschriftenbibliothek EZB, Open J-Gate, OCLC WorldCat, Universe Digital Library, NewJour, Google Scholar

